Mictomagnetic, ferromagnetic, and antiferromagnetic transitions in $La(Fe_xAl_{1-x})_{13}$ intermetallic compounds

T. T. M. Palstra, G. J. Nieuwenhuys, and J. A. Mydosh
Kamerlingh Onnes Laboratorium der Rijks-Universiteit Leiden, 2300-RA Leiden, The Netherlands

K. H. J. Buschow
Philips Research Laboratories, 5600-JA Eindhoven, The Netherlands

(Received 8 June 1984)

Cubic $La(Fe_xAl_{1-x})_{13}$ intermetallic compounds can be stabilized with iron concentration x between 0.46 and 0.92 in the $NaZn_{13}$-type structure ($D2_3$) with $Fm3c$ (O_h^6) space-group symmetry. Here the Fe-Fe coordination number can increase up to 12. At low x values, a mictomagnetic regime occurs with distinct cusps in the ac susceptibility. With the increase of the iron concentration, a soft ferromagnetic phase is found which at lower temperatures shows anisotropy effects related to reentrant mictomagnetic behavior. Finally, for $x > 0.86$, antiferromagnetic order appears along with a sharp metamagnetic transition in external fields of a few teslas. The saturation magnetic moment increases linearly with x from $1.4\mu_B$/Fe to $2.1\mu_B$/Fe throughout the ferromagnetic and antiferromagnetic regime. The breakdown of long-range ferromagnetic order at high x values can be explained by modifications of the iron moment and their coupling at a large Fe-Fe coordination number. However, with application of a magnetic field, the ferromagnetic state can be fully recovered. The room-temperature resistivity decreases with increasing x from 200 to 160 $\mu\Omega$ cm. The low-temperature slope $d\rho/dT$ is related to the magnetic order, being negative in the antiferromagnetic state and positive in the ferromagnetic state. The metamagnetic transition causes a decrease of the resistivity of about 20% and a sign change in $d\rho/dT$. This behavior is discussed in terms of the two-current model. The thermal expansion exhibits a strong Invar character and is described by a combined band and local-moment model which allows calculations of corresponding magnetovolume coupling constants. The metamagnetic transition causes a large magnetic striction.

I. INTRODUCTION

Recently we have succeeded in fabricating several cubic $NaZn_{13}$-type ($D2_3$) pseudobinary compounds of the formula $La(Fe_xSi_{1-x})_{13}$ and $La(Fe_xAl_{1-x})_{13}$. We previously reported results for the former compound, which exists in the small x range between 0.81 and 0.88.[1] Here we found the Invar characteristic that the Curie temperature decreases with increasing iron moment. Also we observed a strong critical behavior in the temperature dependence of the magnetization, susceptibility, and resistivity. The ferromagnetic state had a susceptibility critical exponent corresponding to the value for a three-dimensional Heisenberg ferromagnet.

We now present ac susceptibility, magnetization, electrical resistivity, and magnetostriction measurements of $La(Fe_xAl_{1-x})_{13}$, which can be stabilized over a much larger x range, between $x=0.46$ and $x=0.92$. Here we observe with increasing iron concentration mictomagnetic, ferromagnetic, and antiferromagnetic regimes, respectively. Furthermore, it is possible to recover the full ferromagnetic state from the antiferromagnetic state by applying a magnetic field of a few teslas, i.e., a metamagnetic transition.[2] Thus we can investigate the behavior of the electrical resistivity and spontaneous magnetostriction of an intermetallic compound either in the antiferromagnetic or ferromagnetic state by means of a magnetic field. Mössbauer spectroscopy[3] shows a continuously increasing effective hyperfine field at the iron nucleus for $0.54 < x < 0.85$.

The $La(Fe_xAl_{1-x})_{13}$ system can be compared to Fe_xAl_{1-x} (Refs. 4 and 5) at low x values, and a number of similarities exist in the magnetic behavior. An extremely interesting extension occurs at the high x values. In Fe_xAl_{1-x} the Fe-Fe coordination number can be increased up to 8. However, $La(Fe_xAl_{1-x})_{13}$ is one of the few iron-based systems in which the Fe-Fe coordination number can increase up to 12 without being troubled by structural (martensitic) phase transformations. For this system we observe the breakdown of long-range ferromagnetic order at large Fe-Fe coordination numbers. From our measurements we can track the formation of the Fe magnetic moments with increasing x and determine the complete magnetic phase diagram. In addition we have studied the magnetic field, temperature, and iron concentration dependence of the metamagnetic transition.[2] This spin-flip transition is rather unique for cubic intermetallic compounds, since it is very sharp, occurs at low fields, and exhibits large hysteresis effects.

In Sec. II we give the experimental details of our sample preparation and measuring techniques. Section III contains the experimental results. In Sec. IV these results are discussed and compared with other Fe-based systems, and finally the main conclusions are presented in Sec. V.

II. EXPERIMENTAL PROCEDURES

The $La(Fe_xAl_{1-x})_{13}$ samples were prepared by arc melting in an atmosphere of ultrapure argon gas. The

purities of the three starting elements were all better than 99.9%. After repeated arc melting the samples were annealed for about 10 days at 900°C. X-ray diffraction analysis showed that single-phase samples of the $NaZn_{13}$ type of structure were obtained in the concentration region between $x=0.46$ and 0.92.

The low-field ac susceptibility was measured by means of a sensitive mutual inductance technique operating at a frequency of 118 Hz with a driving field of less than 0.1 mT. The temperature was varied stepwise and determined to within 0.2% by means of calibrated carbon-glass and platinum resistors. The samples were spark cut from the bulk into perfect spheres. Magnetization was measured using a vibrating sample magnetometer operating at a frequency of 21 Hz. Magnetic fields up to 5 T were produced by a superconducting solenoid. The high-field (35 T) magnetization experiments were performed at 4.2 K in the high-field magnet at Amsterdam.[6]

The resistivity between 4 and 300 K was measured by means of a standard four-point probe technique with a dc current of 10 mA. The resistivity samples were spark cut from the bulk and had typical dimensions of $1\times1\times15$ mm^3. The electrical leads were attached with silver paint. The temperature was increased stepwise and determined to within 0.2% again using calibrated carbon-glass and platinum resistors. A constant dc field up to 7 T could be applied by means of a superconducting solenoid perpendicular to the measuring current. The relative accuracy of the resistivity was about 1 part in 10^5 and the error in the absolute value was about 3% due to uncertainties in the sample dimensions.

Thermal-expansion measurements were carried out between 6 and 300 K by means of a three-terminal capacitance technique, using a dilatometer similar to that described by Brändli and Griessen.[7] The samples were spark cut from the bulk and had typical dimensions of $4\times4\times4$ mm^3. The temperature was increased in steps of 10 K in a continuous flow cryostat and determined with a calibrated constant linear temperature sensor to better than 0.2 K. The length changes were measured relative to Berylco 25 out of which the dilatometer was constructed. Corrections for the length changes of the dilatometer were made by measuring the thermal expansion of 99.999% Cu of the same dimensions and comparing the results with the thermal-expansion data of Cu given by Hahn.[8] Magnetostriction at 4.2 and 77 K was measured by immersing the dilatometer in liquid helium or nitrogen. This cryostat was then placed inside another one containing a 12-T superconducting solenoid. The magnetic field was varied in small steps and a correction for the dielectrical constant of helium or nitrogen was taken into account.

III. EXPERIMENTAL RESULTS

A. Zero-field measurements

The magnetic phase diagram for $La(Fe_xAl_{1-x})_{13}$ can be divided into three x regimes as distinguished by the behavior of the ac susceptibility, resistivity, and magnetization. In Fig. 1 we show a typical example for the susceptibility of each regime. The susceptibility is plotted in

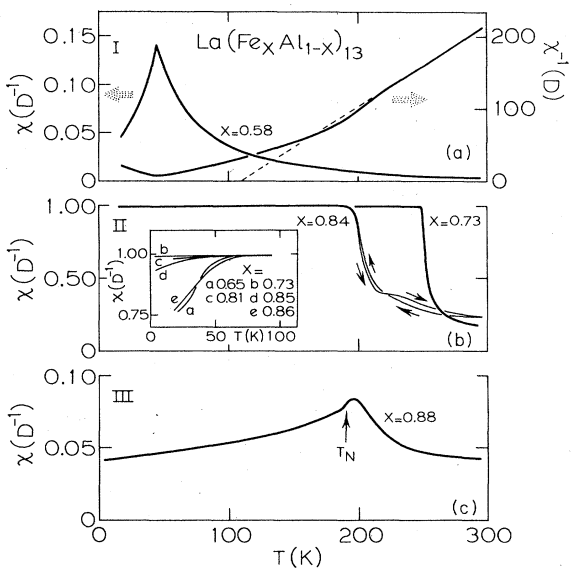

FIG. 1. Temperature dependence of the low-field ac susceptibility for the three regimes of $La(Fe_xAl_{1-x})_{13}$. (a) In regime I, we show a typical mictomagnetic behavior; (b) in regime II, a ferromagnetic transition; (c) in regime III, an antiferromagnetic one. The inset in (b) shows the low-temperature deviations from the soft ferromagnetic state. Note the different χ scales.

units of the inverse demagnetizing factor D^{-1} ($D=4\pi/3$ for a sphere), thus yielding 1.00 for a soft ferromagnet. In the first regime (I), $0.46\leq x<0.62$, the behavior of the susceptibility is characterized by a sharp cusp at about 50 K, indicative of mictomagnetism (i.e., a random freezing of ferromagnetic clusters). Figure 1(a) shows the susceptibility of a $x=0.58$ sample along with the inverse susceptibility. The large positive Curie-Weiss temperature intercept, $\Theta=+110$ K, indicates the presence of predominantly ferromagnetic exchange interactions. Deviations from Curie-Weiss behavior start from 230 K which is about 5 times the freezing temperature, $T_f=44.5$ K. The susceptibility increases rapidly with increasing x, reaching 0.25% of D^{-1} at T_f for $x=0.46$, 1.1% for $x=0.54$, and 14% for $x=0.58$, respectively.

The susceptibility in the second regime (II), $0.62<x\leq0.86$, exhibits soft ferromagnetic behavior. The Curie temperature first increases with x up to a maximum $T_C=250$ K for $x=0.75$ and then decreases. At lower temperatures the susceptibility deviates from the inverse demagnetizing factor D^{-1} limit [see inset of Fig. 1(b)]. These deviations are the smallest for the samples with the highest T_C. This means that the soft ferromagnetic state is being destroyed and a reentrant mictomagnetic state is probably appearing.[9] In a small interval, $0.84<x<0.86$, a slight hysteresis has been observed at high temperatures. Here the susceptibility above T_C behaves differently when heating and cooling. Yet both curves yield the same T_C, which is defined in Fig. 1(b) as the intercept of the two straight lines extrapolated from just above and below T_C.

In the third regime (III), $0.86<x\leq0.92$, the susceptibility has an antiferromagnetic character. The broad maximum in the susceptibility for all samples is about

10% of D^{-1}. Only at the concentration limit $x=0.92$ does the susceptibility obtain a value of about 80% of D^{-1}. This is probably due to a second phase that has been observed at the grain boundaries and in the x-ray spectrum and probably consists of pure α(bcc)-Fe. The Néel temperatures, defined as the maximum in $d(T\chi)/dT$, increase with increasing x. Here also hysteresis at high temperatures has been observed in the limited concentration region $0.91<x<0.92$.

The temperature dependence of the total resistivity is displayed in Fig. 2 for typical examples of all three regimes. The general trend is that the room-temperature resistance decreases from 200 $\mu\Omega$ cm for $x=0.58$ down to 157 $\mu\Omega$ cm for $x=0.91$. In regime I we observe a negative $d\rho/dT$ at low temperatures. The slope increases with increasing x but remains negative up to the low x part of regime II. For $x=0.73$ the relative change in resistance between helium and room temperature is less than 0.3%. For $x\geq 0.77$ the slope $d\rho/dT$ is positive. In regime III $d\rho/dT$ becomes negative again.

Large anomalies in the resistance are observed around the magnetic ordering temperatures. In order to elucidate these anomalies we have plotted $d\rho/dT$ versus T in Fig. 3. In the mictomagnetic regime (I) no anomaly is observed around T_f. In the ferromagnetic regime (II) a negative cusp develops around T_C and increases in magnitude with increasing x until a sharp minimum is reached for $x=0.84$. The ferromagnetic $x=0.86$ sample deviates from all other concentrations by having a λ-shaped anomaly. Finally in the antiferromagnetic regime (III) a sharp negative cusp is found again.

Figure 4 shows the spontaneous volume magnetostriction $\omega_s=\Delta V/V=3\,\Delta l/l$ versus the temperature (T) and the reduced temperature (T/T_C). Three samples were measured in the ferromagnetic regime (II) and one in the antiferromagnetic regime (III). The spontaneous volume

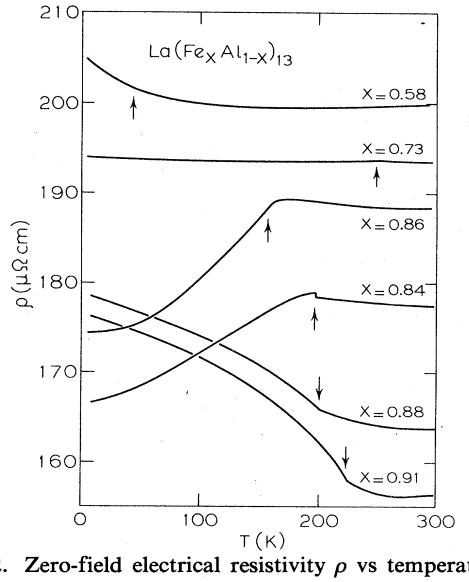

FIG. 2. Zero-field electrical resistivity ρ vs temperature for La(Fe_xAl_{1-x})$_{13}$. The arrows indicate the magnetic ordering temperatures.

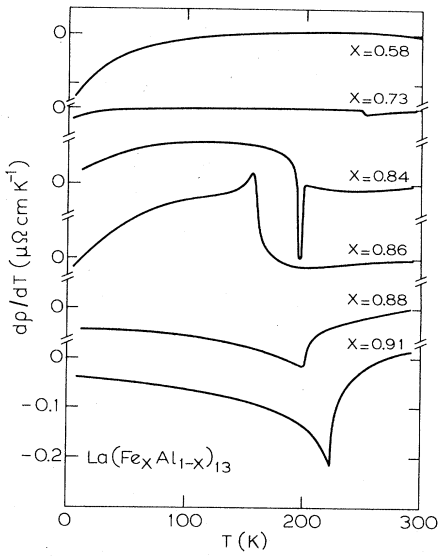

FIG. 3. Temperature derivative of electrical resistivity $d\rho/dT$ vs temperature for La(Fe_xAl_{1-x})$_{13}$.

magnetostriction ω_s is obtained by subtracting a Grüneisen function, defined by the linear high-temperature (300 K) slope of $\Delta l/l$, or $\alpha_t=13\times10^{-6}\,\mathrm{K}^{-1}$, and a Debye temperature $\Theta_D=300$ K, from the observed thermal expansion.[10] These values of α_t and Θ_D seem to be appropriate for all samples. The always-negative slope of the magnetic ω_s, shown in Fig. 4, clearly indicates the Invar character of the La(Fe_xAl_{1-x})$_{13}$ intermetallic compounds. For $x=0.65$ a zero total thermal-expansion coefficient $\alpha_t=l^{-1}\,dl/dT$ has been found at 140 K, and for the other three samples this takes place at about 240 K. Usually, the negative magnetic thermal-expansion coefficient is related to the increase of the magnetic correlation function as the temperature is lowered.[11] This also seems to occur in the antiferromagnetic region. Figure 4 further shows that the magnetic moments originate far above T_C.

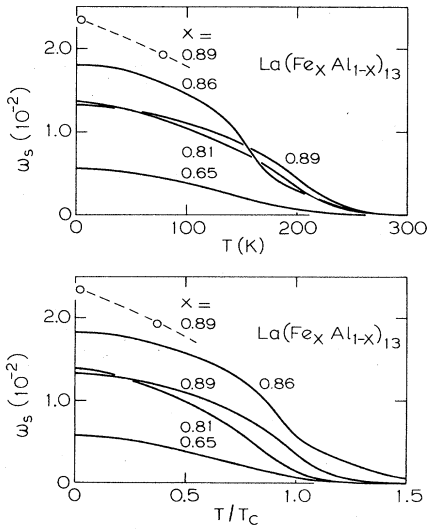

FIG. 4. Spontaneous volume magnetostriction ω_s vs temperature T and reduced temperature T/T_C.

B. Field measurements

In Fig. 5 we show the field dependences of the magnetization at 4.2 K. In the first regime, $0.46 \leq x < 0.62$, it was not possible to saturate the magnetization in fields up to 5 T and an "*S*-shaped" *M-H* curve was found, typical of the mictomagnetic state. Regime II, $0.62 < x \leq 0.86$, exhibits a soft ferromagnetic state with a remanent magnetization less than 1% of the saturation magnetization. In the third regime, $0.86 < x \leq 0.92$, the magnetization increases only slowly with increasing field until at moderate fields a sharp spin-flip transition is found to the fully saturated ($2.2\mu_B$/Fe) moment. This transition takes place within 1 mT, which is our measuring accuracy.

Figure 5(c) exhibits the measured magnetization curves for $x = 0.88$ as a typical example for the third regime. All samples were cooled in zero field to helium temperature and then the magnetic field was increased. The spin-flip field at $x = 0.88$ and 4.2 K, measured with increasing field, is 3.88 T, but only 0.61 T with decreasing field. The width of the hysteresis loop decreases with increasing temperature. The metamagnetic transition fields increase with increasing x up to 13.5 T for $x = 0.92$ and the hysteresis width becomes larger with increasing x.[2]

Figure 6 shows the saturation moments per Fe atom of all three regimes. The magnetic moment increases linearly with x in regimes II and III having a slope of $0.24\mu_B$/Fe resulting in $2.4\mu_B$/Fe for the hypothetical compound $LaFe_{13}$. In regime I there are deviations from this line because it is not possible to saturate the magnetization in fields up to 5 T. In regime II the magnetization is saturated in fields directly above the demagnetizing field and no increase of the magnetization is observed in fields up to 20 T. For regime III we have determined the saturation magnetic moments in fields above the spin-flip field.

In Fig. 7 we show the resistivity of a $x = 0.88$ sample in a field of 4.76 T, along with the zero-field resistance as a typical example of the antiferromagnetic regime (III). Upon applying a field at helium temperature, the resistivity $\rho(H)$ first decreases at a rate 1 $\mu\Omega$ cm/T and at the spin-flip transition there is a $\Delta\rho$ of 20 $\mu\Omega$ cm for the $x = 0.88$ sample. Thus, there is a total decrease of the resistivity in a field of 4.76 T of about 17%. Furthermore, the negative $d\rho/dT$ in zero field becomes positive beyond the spin-flip field. Above T_N there is no observable field dependence of the resistivity. The magnetoresistance of the spin-flipped antiferromagnetic samples (III) is quite similar to the zero-field resistance of the ferromagnetic samples (II). Samples in the ferromagnetic regime (II) do not show pronounced changes upon applying a magnetic field.

In order to further elucidate the anomalies around T_N, we have plotted $d\rho/dT$ versus T for both zero field and a 4.8-T field in Fig. 8. In both cases a sharp negative peak

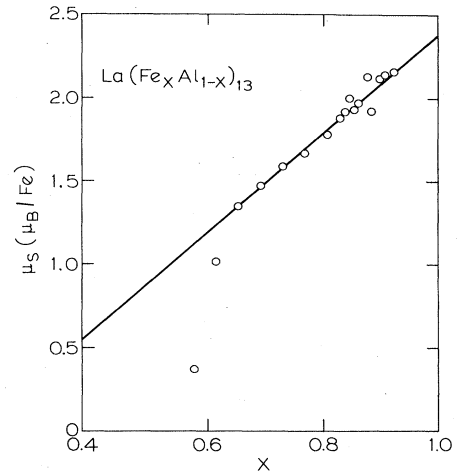

FIG. 6. Saturation magnetic moments of $La(Fe_xAl_{1-x})_{13}$ as a function of x.

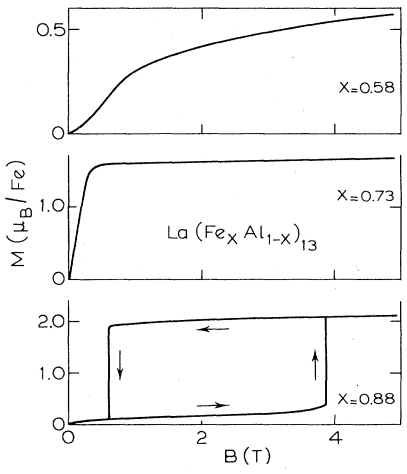

FIG. 5. Magnetization as a function of magnetic field for the three regimes of $La(Fe_xAl_{1-x})_{13}$ at helium temperature. In Regime I we show the behavior of a mictomagnet; in regime II, of a ferromagnet; and in regime III we show the metamagnetic behavior of the antiferromagnetic regime for an $x = 0.88$ sample.

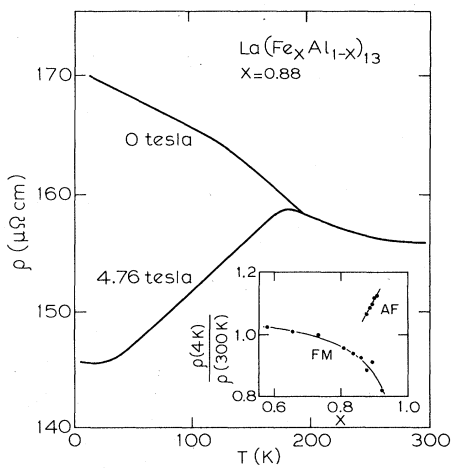

FIG. 7. Electrical resistivity ρ vs temperature for an antiferromagnetic $La(Fe_xAl_{1-x})_{13}$ sample ($x = 0.88$) in zero field and in a field $H = 4.76$ T greater than the spin-flip field H_{sf}. The inset shows the ratio $\rho(4\text{ K})/\rho(300\text{ K})$ vs iron concentration x. FM indicates the ferromagnetic or induced ferromagnetic state and AF the antiferromagnetic ground state.

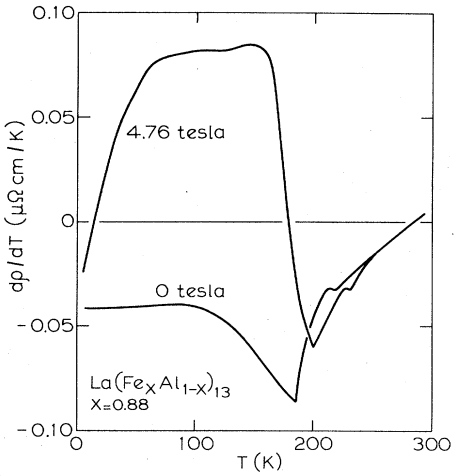

FIG. 8. Temperature derivative $d\rho/dT$ vs temperature for an antiferromagnetic La(Fe$_x$Al$_{1-x}$)$_{13}$ sample ($x=0.88$) in zero field and in a field $H=4.76$ T ($H>H_{sf}$).

is found at T_N. In regime III we have used exactly this criterion to define T_N. The theoretical T_N definition, namely the maximum in $d(\chi T)/dT$, is not as well defined because the zero-field susceptibility in this regime shows a rather smooth transition. Figure 8 also illustrates that the magnetic ordering temperature T_N increases 14 K by applying a field of 4.76 T. In both curves there is a second anomaly above T_N whose origin is not clear. This anomaly also shifts in temperature upon applying a field.

In Fig. 9 we display the magnetostrictive effects of a $x=0.89$ sample at 4.2 K. The behavior of the other samples in the antiferromagnetic regime (III) is analogous. Up to the spin-flip transition the relative volume change ω_f is rather small ($\omega_f=6\times10^{-4}$). At the spin-flip transition there is a huge magnetic expansion ($\omega_f=+1\times10^{-2}$). Upon decreasing the field the same hysteresis loop is followed, as has been observed with the magnetization [see Fig. 5(c)]. The nonreversibility at low fields is due to the

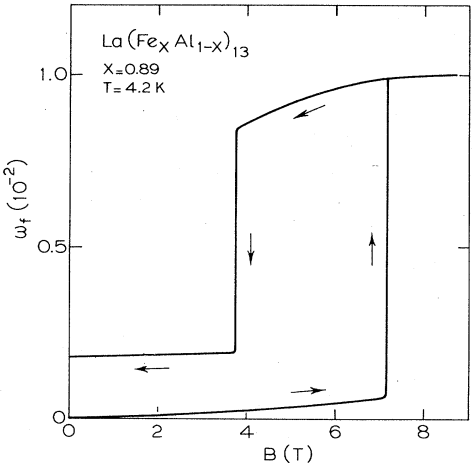

FIG. 9. Forced volume magnetostriction $\omega_f=\Delta V/V$ as a function of magnetic field for an antiferromagnetic La(Fe$_x$Al$_{1-x}$)$_{13}$ sample ($x=0.89$) at helium temperature.

appearance of visible cracks in the sample. To reduce this irreversibility the sample can be previously cycled at helium temperature in a magnetic field before ω_f versus H is measured. At 77 K the magnitude of the expansion at the spin-flip transition decreased to $\omega_f=+7.2\times10^{-3}$ and the hysteresis width decreased from 3.5 T at 4.2 K to 0.5 T at 77 K.

IV. DISCUSSION

A. Crystal structure, composition, and stability

La(Fe$_x$Al$_{1-x}$)$_{13}$ has the cubic NaZn$_{13}$ ($D2_3$) structure with $Fm3c$ (O_h^6) space-group symmetry. In the hypothetical compound LaFe$_{13}$ the Fe atoms occupy two different sites Fe$^{\rm I}$ and Fe$^{\rm II}$, in a ratio 1:12. In Wijckoff notation these sites are designated by the symbols 8(b) and 96(i), each unit cell comprising 8 formula units LaFe$_{13}$. The La and Fe$^{\rm I}$ atoms from a CsCl ($B2$) structure. Additionally the La atoms are surrounded by a polyhedron of 24 Fe$^{\rm II}$ atoms. The Fe$^{\rm I}$ atoms are surrounded by an icosahedron of 12 Fe$^{\rm II}$ atoms and the Fe$^{\rm II}$ atoms are surrounded by 9 nearest Fe$^{\rm II}$ atoms and 1 Fe$^{\rm I}$ atom, see Fig. 10 and inset of Fig. 11. This Fe$^{\rm I}$-Fe$^{\rm II}$ distance (d), being only 2% shorter than the Fe$^{\rm II}$-Fe$^{\rm II}$ distance, decreases, as does the lattice parameter (a), linearly with x from 2.510 Å for $x=0.46$ to 2.431 Å for $x=0.92$. This behavior for d and a is shown in Fig. 11.

The heat of alloying between La and Fe is positive because there exist no stable La-Fe intermetallics. Thus a minimum amount of Al is required to create a negative heat of formation and a pseudobinary compound can be stabilized with a suitable structure to accomodate the atomic radii of all three constituents. When substituting Al for Fe, the NaZn$_{13}$ structure is adopted in the concen-

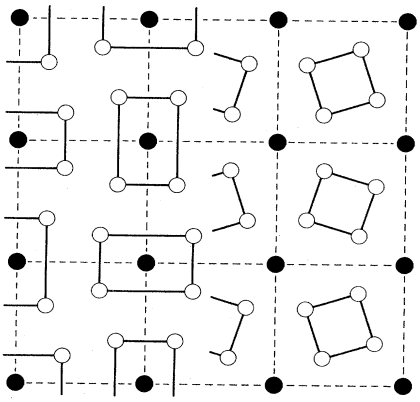

FIG. 10. The $z=0$ plane of the hypothetical compound LaFe$_{13}$. Fe$^{\rm I}$ is denoted by ● and Fe$^{\rm II}$ by ○. The complete iron sublattice can be obtained by cubic symmetry. The La atoms occupy the $(\frac{1}{4},\frac{1}{4},\frac{1}{4})$ sites plus their symmetry operations. The solid lines on the right-hand side of the figure connect the $6\times4=24$ nearest neighbors of La, and on the left-hand side they connect the $3\times4=12$ nearest neighbors of Fe$^{\rm I}$. One unit cell contains 8 formula units.

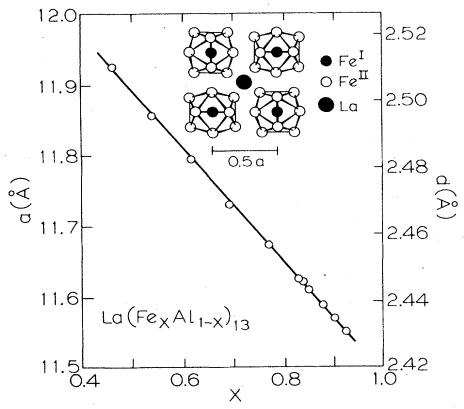

FIG. 11. Dependence of the lattice constant a on Fe concentration in $La(Fe_xAl_{1-x})_{13}$. The right-hand scale refers to the distance d between the Fe^I and Fe^{II} atoms. The inset shows a projection along the c axis for a part of the $NaZn_{13}$-type unit cell.

tration region $0.46 \leq x \leq 0.92$. By substituting Si for Fe, this stable concentration region is much smaller, viz., $0.8 \leq x \leq 0.9$.[1] When the Al concentration becomes too large, another structure, $LaFe_4Al_8$, is favored. On the low-Al-concentration side the compound is not stable with respect to pure α-Fe; $LaFe_{13}$ does not exist. On the other hand, the heat of alloying for La and Co is already negative since the intermetallic compound $LaCo_{13}$ (Curie temperature $T_C = 1290$ K) and several other La_xCo_y intermetallics do exist.[12] For $La(Co_xSi_{1-x})_{13}$ the $NaZn_{13}$ structure is stable for $0.8 \leq x \leq 1.0$. For La-Ni intermetallics almost the same situation occurs as for La-Fe. $LaNi_{13}$ is not stable and no intermetallics are found between pure Ni and the Haucke-phase $LaNi_5$. Here also, substitution of Ni by Al or Si is required to stabilize the $NaZn_{13}$ structure.

The occupation of the Fe^I and Fe^{II} sites by Fe and Al does not proceed in a random way. Neutron scattering experiments on $La(Fe_xAl_{1-x})_{13}$ samples with $x = 0.69$ and 0.91 indicated that the Fe^I site is fully occupied by Fe.[13] Thus a considerable amount of Fe atoms will have a fcc-like local environment with 12 nearest neighbors. The Fe^{II} sites are distributed randomly by the remainder of the Fe and Al atoms. This means that the mean Fe-Fe coordination number for both Fe^I and Fe^{II} sites can vary from 4.8 for $x = 0.46$ to 9.4 for $x = 0.92$.

B. Magnetic properties

The magnetic phase diagram of $La(Fe_xAl_{1-x})_{13}$ can be constructed from the results of the susceptibility, resistivity, and magnetization experiments. The first regime (I), $0.46 \leq x < 0.62$, consists of a mictomagnetic state with a distinct cusp in the ac susceptibility and an S-shaped magnetization curve. Upon increasing the iron concentration x, we find a soft ferromagnetic state in regime II, $0.62 < x \leq 0.86$. Finally, at the highest iron concentration, $0.86 < x \leq 0.92$, an antiferromagnetic state exists, with a sharp metamagnetic transition in a magnetic field of a few teslas. The experimental phase diagram of $La(Fe_xAl_{1-x})_{13}$ is constructed from the magnetic ordering temperatures and displayed in Fig. 12.

For $x < 0.75$ there are striking similarities between $La(Fe_xAl_{1-x})_{13}$ and Fe_xAl_{1-x}. Although the crystal structure is different, they both are cubic. Furthermore, we find a mictomagnetic phase in $La(Fe_xAl_{1-x})_{13}$ for $x < 0.6$, whereas Fe_xAl_{1-x} also has a mictomagnetic phase for $x < 0.73$.[4] This means that both compounds become mictomagnetic when the average number of nearest-neighbor Fe atoms is less than 6.0, even though the local environments of the Fe atoms and the lattice parameters are different. Recently, a semiquantitative model has been proposed for the phase diagram of Fe_xAl_{1-x}.[5] We believe that the main ideas of this model are also applicable to $La(Fe_xAl_{1-x})_{13}$. Here it was proposed that mictomagnetic behavior arises by virtue of competition between a nearest-neighbor Fe-Fe ferromagnetic exchange and a further-neighbor Fe-Al-Fe antiferromagnetic superexchange. With such coupling the magnetic moments will be frozen-in below the freezing temperature T_f in random orientations without long-range ferromagnetic or antiferromagnetic order, i.e., a mictomagnetic cusp appears in the low-field susceptibility. Short-range ferromagnetic order (clustering) causes the deviations from Curie-Weiss behavior up to $5T_f$ and the large positive Curie-Weiss temperature $\Theta = +110$ K. It has been shown in Fe_xAl_{1-x} that the magnetic moment of Fe is strongly dependent upon the number of nearest-neighbor (NN) Fe atoms.[14] In Fe_xAl_{1-x} the moment is about $2.2\mu_B$ for Fe atoms having more than five NN Fe atoms. When the number of NN Fe atoms is less than five, the magnetic moment decreases and is zero when this number is less than four. Thus, by decreasing the iron concentration, more and more iron atoms will loose their magnetic moment, thereby decreasing the number of both ferromagnetic and antiferromagnetic interactions, and eventually leading to Pauli paramagnetism. For $La(Fe_{1-x}Al_x)_{13}$ this model explains the decrease in the magnitude of the susceptibility at T_f with decreasing x as well as the behavior of the saturation magnetic moments versus x illustrated in Fig. 6.

Upon increasing the iron concentration above $x = 0.6$,

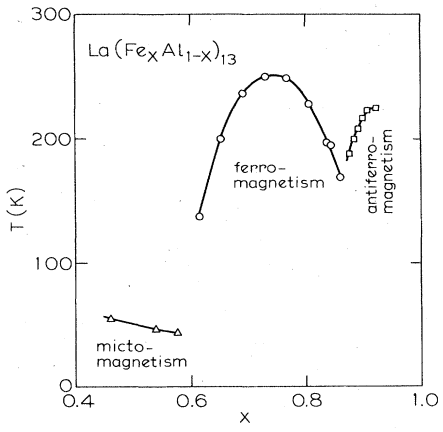

FIG. 12. Magnetic phase diagram of $La(Fe_xAl_{1-x})_{13}$. The cusp temperature is indicated by △, the Curie temperature by ○, and the Néel temperatures by □.

long-range ferromagnetic order is found. Here the Curie temperature increases with increasing x because the number of NN ferromagnetic exchange pairs increases at the cost of the antiferromagnetic superexchange, and because the lattice parameter decreases. The latter argument is supported by hyperfine-field and saturation magnetization measurements,[15] and recent neutron scattering experiments on a variety of Fe-based alloys.[16] These measurements showed that in our range of Fe-Fe distances the exchange constant is positive and increases with decreasing Fe-Fe distance. This result is consistent with the higher T_C values of $La(Fe_xSi_{1-x})_{13}$ compared to $La(Fe_xAl_{1-x})_{13}$ as the lattice parameter of the former compound is smaller.[1] However, upon increasing the iron concentration above $x=0.75$, the Curie temperature begins to decrease and for $x>0.86$ antiferromagnetic order appears. This unexpected collapse of long-range ferromagnetic order with increasing iron concentration has long been studied in connection with γ-Fe (fcc) and Fe_xNi_{1-x} alloys in the Invar region (fcc, $x\approx 0.65$).

Calculations within the Hartree-Fock approximation (HFA) for the impurity states in ferromagnetic transition metals show that an Fe impurity in a ferromagnetic host has two stable solutions, crucially depending on the local environment.[17] One solution, Fe(I), corresponds to a magnetic moment m_{I}, parallel to the bulk magnetization. The other solution, Fe(II), represents a magnetic moment m_{II} antiparallel to the bulk (host) magnetization. The ratio of Fe(I) to Fe(II), which depends on the local environment, can be determined by minimizing the total energy.[18] This model has been extended to concentrated alloys and it has been argued that when the iron concentration increases beyond a certain limit, the Fe(II) solution becomes stabilized.[17] Furthermore, it was suggested that even when a small fraction of the atomic moments is antiparallel to the magnetization, the ferromagnetic state can be unstable.[19] However, it is not clear what the resulting magnetic ground state will be in such an alloy after the collapse of long-range ferromagnetic order. Many years ago Weiss[20] introduced a two-level model for γ-Fe, based on low-temperature measurements. Here there is a low-volume, low-magnetic moment ($0.5\mu_B$/Fe) antiferromagnetic ground state, and a thermally excited upper level with a high-volume and high magnetic moment ($2.8\mu_B$/Fe) ferromagnetic state. This model is in many respects similar to the results obtained by the HFA calculations. Unfortunately, fcc-Fe only exists, under normal pressures, at high temperatures where no long-range order of the magnetic moments occurs. Nevertheless, this model was used by other authors in order to explain the magnetic behavior of Fe-Ni Invar alloys.[21,22] Neutron scattering experiments on such alloys have revealed a negative Fe-Fe exchange constant, but an antiferromagnetic state has not been found due to an $\gamma\rightarrow\alpha$ martensitic-crystallographic transformation. This antiferromagnetic state has indeed been found in Fe-Ni-Mn alloys where the $\gamma\rightarrow\alpha$ martensitic transition can be suppressed.[23].

We believe that the collapse of long-range ferromagnetic order in $La(Fe_xAl_{1-x})_{13}$ at the highest iron concentration, $0.86<x\leq 0.92$, is of the same origin as in Fe-Ni, Fe-Ni-Mn, and γ-Fe. In this concentration range a considerable portion of Fe^{I} sites has a Fe-Fe coordination number approaching 12, and a considerable number of Fe^{II} sites up to 10. Here, at these high coordination numbers, the Fe(II) state becomes stabilized and when a finite fraction Fe atoms occupies this state, the ferromagnetic order collapses. However, for $La(Fe_xAl_{1-x})_{13}$ the ferromagnetic state can be recovered by applying a magnetic field.

It was suggested that the instability of the Fe(I) state originates in iron-rich environments, before the collapse of long-range ferromagnetic order.[19] Furthermore, this instability of the ferromagnetic state should be accompanied by fluctuations of the now weakly coupled magnetic moments. Then, near the critical concentration, these fluctuations must be taken into account, and cause the Fe moments to form a low-temperature asperomagnetic state, i.e., disordered, noncollinear ferromagnetic state.[17] This corresponds with the decrease of the low-field susceptibility from D^{-1} at low temperature for $0.81\leq x\leq 0.86$ [see inset of Fig. 1(b)].

Although the magnetic structure of the antiferromagnetic phase has not yet been investigated, we expect that due to the random occupation of the Fe^{II} sites by Fe and Al, a highly inhomogeneous magnetic state originates with ferromagnetic iron-poor clusters coupled antiferromagnetically by iron-rich clusters. It can be inferred from the extremely large resistivity that the antiferromagnetic state is highly disordered. By increasing the magnetic field, the Fe(I) state is favored, thereby further increasing the internal field. As soon as the internal field passes a critical value, a sharp spin flip is observed in which all moments are orientated along the field axis.

The *linear* decrease of the saturation magnetic moment with decreasing iron concentration down to $1.35\mu_B$/Fe remains rather peculiar (see Fig. 6). Notwithstanding, the saturation moments of $La(Fe_xSi_{1-x})_{13}$ also lie along this line. Only for low concentrations of nonmagnetic elements dissolved in Fe is a linear decrease of the magnetic moment of Fe observed and explained within the rigid-band model.[24] However, without detailed band-structure calculations for our compounds, we cannot say if the assumptions of this model are in agreement with the real band structure over such a large x region of compounds.

C. Electrical resistivity

The main features of the electrical resistivity of $La(Fe_xAl_{1-x})_{13}$ are (i) the resistivity is large ($>150\ \mu\Omega$ cm), (ii) in region III (antiferromagnetic ordering) a negative $d\rho/dT$ is found over the whole temperature range, and (iii) critical effects are observed around the transition temperature.

The large resistance suggests that Mooij's rule[25] may be applied which describes the effects of various types of disorder on the electrical resistivity of transition-metal alloys. This rule states that in a wide T range around room temperature, the temperature dependence of ρ is approximately linear with a temperature coefficient $\alpha_r\equiv\rho^{-1}d\rho/dT$ which is small and changes its sign systematically from positive in alloys with $\rho<100\ \mu\Omega$ cm to negative for $\rho>200\ \mu\Omega$ cm.

In the first two regimes (I and II), $x<0.86$, this rule seems to hold. With increasing ρ the temperature coefficient α_r decreases and $d\rho/dT$ changes from positive for $\rho<190\ \mu\Omega\,\mathrm{cm}$ to negative for $\rho>190\ \mu\Omega\,\mathrm{cm}$. However, in the third regime (III) the room-temperature resistance ($160\ \mu\Omega\,\mathrm{cm}$) is less than in the first two regimes, and yet a negative $d\rho/dT$ is found here. We have keep in mind that although Mooij's rule does not explicitly treat magnetic scattering, it should still be valid in the paramagnetic high-temperature range. We have investigated two samples in this range up to 700 K and found $\alpha_r=83$ ppm K^{-1}, $\rho=182\ \mu\Omega\,\mathrm{cm}$ for $x=0.84$ and $\alpha_r=154$ ppm K^{-1}, $\rho=163\ \mu\Omega\,\mathrm{cm}$ for $x=0.91$, in agreement with Mooij's rule. In addition we found no indication of saturation in $\rho(T)$ at high temperatures.[26]

$La(Fe,Al)_{13}$ enables us to measure the electrical resistivity in the antiferromagnetic ground state as well as in the field-induced ferromagnetic state. In Fig. 7 the experimental results are shown. They may be explained by using the two-current model. For a full description of the validity and range of this model we refer to Dorleijn[27] and Campbell and Fert.[28] This model considers transition metals which are magnetic, e.g., Fe, Co, and Ni. In a ferromagnetic metal it is appropriate to distinguish the electrons according to the direction of their magnetic moment, viz., either parallel or antiparallel to the magnetization within a domain. We indicate the charge carriers with magnetic moment parallel to the magnetization with "up" or ↑, and those antiparallel with "down" or ↓. As was suggested by Mott,[29] scattering events with conservation of spin direction are much more probable at low temperature (i.e., $T\ll T_C$) than scattering events in which the spin direction is changed. Mott's suggestions lead to a description of the conduction by two independent currents in parallel. Since the Fermi surfaces for ↑ and ↓ electrons can be very different there is no reason to assume equal relaxation times or conductivities for the two spin currents. Indeed, a different resistance has been found for the two spin currents in Al dissolved in Fe, $\rho_\downarrow=48\ \mu\Omega\,\mathrm{cm/at.\%}$ Al and $\rho_\uparrow=5.6\ \mu\Omega\,\mathrm{cm/at.\%}$ Al. If we adopt the above values for $LaFe_{13}$, instead of pure Fe, we can calculate the excess resistivity of the antiferromagnet relative to ferromagnet. When replacing 10% of Fe in $LaFe_{13}$ by Al, $La(Fe_{0.9}Al_{0.1})_{13}$, the above-mentioned model gives a magnetic contribution to the resistance in the ferromagnetic state of

$$\rho=\frac{\rho_\downarrow\rho_\uparrow}{\rho_\downarrow+\rho_\uparrow}=50\ \mu\Omega\,\mathrm{cm}\ .$$

However, if the ground state changes from ferromagnetic to antiferromagnetic, both currents will be scattered equally and the magnetic contribution to the resistivity is

$$\rho=\tfrac{1}{4}(\rho_\downarrow+\rho_\uparrow)=134\ \mu\Omega\,\mathrm{cm}\ ,$$

since both currents have the same average resistivity $\frac{1}{2}(\rho_\downarrow+\rho_\uparrow)$. This leads to an increased resistivity of 84 $\mu\Omega\,\mathrm{cm}$ in the antiferromagnetic state relative to the ferromagnetic state. We emphasize that our assumptions are oversimplified and that the numerical estimate is only a rough one, since we used the values of Al dissolved in Fe instead of Al dissolved in $LaFe_{13}$. Nevertheless, this model can lead to a basic understanding of the observed phenomena.

Experimentally we find a decrease in resistivity of 25 $\mu\Omega\,\mathrm{cm}$ when applying a field and thereby changing the antiferromagnetic ground state into an induced ferromagnetic state. Upon increasing the temperature, more thermal excitations will be activated, tending to equalize both currents and above T_C only a paramagnetic scattering is left. Our measurements indicate that the magnitude of the paramagnetic spin-disorder scattering lies in between the values for the ferromagnetic and antiferromagnetic scattering. This leads to a positive $d\rho/dT$ for the induced ferromagnetic state and a negative $d\rho/dT$ for the antiferromagnetic ground state. The negative temperature coefficient indicates that the antiferromagnetic state has a very unusual, highly resistive property.

Similar behavior has been observed in $Fe_{0.5}(Ni_xMn_{1-x})_{0.5}$ that can likewise change from ferromagnetic to antiferromagnetism by varying x.[30] Here also, $d\rho/dT$ is smaller in the antiferromagnetic state than in the ferromagnetic state. However, $d\rho/dT$ is positive in both states, indicating that the paramagnetic scattering is stronger than the scattering in both long-range ordered states.

Upon increasing the Al concentration the two-current model leads to an increase in resistivity as observed. At the highest Al concentrations, i.e., in the mictomagnetic state, a similar discussion as given above leads again to a negative $d\rho/dT$ as has been observed.

The critical behavior of the resistivity denoted as the third feature above displays a sharp negative peak in $d\rho/dT$ for the entire ferromagnetic and antiferromagnetic region, except for the borderline case $x=0.86$, which has a λ-shaped anomaly. The total resistivity consists of three parts: a residual part, a part due to phonon scattering, and a part due to spin scattering. This means that the anomalies near T_C must be ascribed to spin scattering and phonon scattering as affected by magnetic strictive effects.

de Gennes and Friedel,[31] Kim,[32] and Fisher and Langer[33] have calculated the critical behavior of the resistivity of a ferromagnet in terms of spin fluctuations. Although the results differ in some respects from each other, they all found a positive peak in $d\rho/dT$ near T_C. Apparently this is not the case in $La(Fe_xAl_{1-x})_{13}$, except for the $x=0.86$ sample. In the $x=0.86$ case a remarkable resemblance is found with other ferromagnets such as Ni, $GdNi_2$, etc.[34] This means that for all other concentrations this positive peak, due to spin fluctuations, must be overwhelmed by another contribution.

Because of the absence of such a λ-shaped peak in the ferromagnet Fe_3Pt, Viard and Gaviolle suggested that the critical scattering of conduction electrons by phonons must be taken into account.[35] They calculated the phonon contribution for Fe_3Pt and found a negative peak for $d\rho/dT$ near T_C arising from the anomalous behavior of the bulk modulus. Since Fe_3Pt and $La(Fe_xAl_{1-x})_{13}$ both have Invar characteristics (see Sec. IV D), we expect that the behavior of the bulk modulus is roughly similar. Thus we propose that an anomalous decrease of the bulk

modulus below T_C leads to the observed negative peaks in $d\rho/dT$ around T_C in $La(Fe_xAl_{1-x})_{13}$. We note that the Curie temperature does not correspond with the temperature at which the peak is observed but always is a bit higher.

Beginning with Suezaki and Mori[36] many authors[37] have calculated the critical behavior of the electrical resistivity of antiferromagnetic metals near T_N. All calculations suggested a large negative peak at T_N due to scattering of the conduction electrons by thermal fluctuations of spins. This is in agreement with the observed behavior of $La(Fe_xAl_{1-x})_{13}$ with $x>0.86$. This negative peak might even be enhanced by the aforementioned critical behavior of the phonon scattering.

D. Spontaneous and forced magnetostriction

The Invar effect has attracted a wealth of interest from both experimentalists and theorists.[38] The archetypical example is Fe_xNi_{1-x} ($x=0.65$), which has a zero thermal-expansion coefficient around room temperature. For $La(Fe_xAl_{1-x})_{13}$ we find a zero thermal-expansion coefficient α_t at 240 K for samples near the instability of long-range ferromagnetic order ($x=0.81$, 0.86, and 0.89). The Invar effect has been explained by a cancellation of the lattice thermal expansion α_1 by a negative magnetic term α_m.[21]

One of the first Invar theories was proposed by Weiss[20] (see Sec. IV B). He suggested a local-moment model with two nearly degenerate states for the Fe atoms, viz., a ferromagnetic ground state and an antiferromagnetic excited state. The latter is characterized by a lower magnetic moment and a smaller atomic volume. By raising the temperature an increasing number of iron atoms will occupy the low-volume excited state, leading to a negative α_m. However, when applied to $La(Fe_xAl_{1-x})_{13}$, this model cannot account for the behavior of the $x=0.89$ sample, which already has an antiferromagnetic ground state and yet α_m is negative.

A more general local-moment volume magnetostriction theory was developed by Callen and Callen.[39] They showed that the spontaneous volume magnetostriction $\omega_s=\Delta V/V$ is given by the two-spin correlation function $\langle \mathbf{m}_i\cdot\mathbf{m}_j\rangle$ as

$$\omega_s=\sum_{i,j}\kappa C_{\rm loc}\langle \mathbf{m}_i\cdot\mathbf{m}_j\rangle ,$$

where κ is the compressibility, $C_{\rm loc}$ a magnetovolume coupling constant, and i,j are the lattice sites. This magnetovolume effect arises from the volume dependence of the exchange integral.

More recently the magnetovolume effect was studied by extending the Stoner band model with volume-dependent terms.[40] This leads to a phenomenological relation, verified for a number of materials:[41]

$$\omega_s=\kappa C_{\rm band}\sum_i m_i^2(T)$$

where $C_{\rm band}$ is the magnetovolume coupling constant due to the band mechanism and $m_i(T)$ is the temperature-dependent local moment on site i as discussed by Shiga,[42] and not the bulk magnetization $M(T)$. Here, the magnetovolume effect can be understood in terms of the increase of the kinetic energy of the electron system due to the splitting of the $3d$ band.[43] The repulsion arises because the electron system can reduce its kinetic energy by undergoing a lattice expansion.

In order to explain the magnetostriction results of $La(Fe_xAl_{1-x})_{13}$, we must consider both a local moment and a band part, by adding both contributions.[42] Below the Curie temperature, in the ferromagnetic state, $\langle \mathbf{m}_i\cdot\mathbf{m}_j\rangle$ and m_i^2 can be approximated by M^2 and this leads to the relation

$$\omega_s(T)=\kappa(C_{\rm loc}+C_{\rm band})M^2(T) .$$

If we compare the saturation magnetization of $La(Fe_xAl_{1-x})_{13}$ (beyond the spin-flip transition for $x=0.89$) with the magnetic contribution of the thermal expansion at helium temperature, we find large positive magnetovolume coupling constants $\kappa C=\kappa(C_{\rm loc}+C_{\rm band})=1.79$, 1.71, and 1.73×10^{-8} cm^6/emu^2 for $x=0.81$, 0.86, and 0.89, respectively. This result, along with the observed resistivity behavior, suggests the equivalence of the ferromagnetic and induced ferromagnetic state. For $x=0.65$, near the mictomagnetic regime, we find an even larger constant $\kappa C=2.09\times10^{-8}$ cm^6/emu^2. These values are about twice as large as for bcc Fe, FeNi Invar, and Fe_3Pt.[41,42]

From these measurements we cannot say whether the band or the local-moment contribution is larger. Shiga[42] calculated that for bcc Fe and FeNi-Invar alloys the band contribution is much larger than the local-moment part at low temperatures: $C_{\rm band}\gg C_{\rm loc}$. Furthermore, self-consisting spin-polarized energy-band calculations[43] have shown that hypothetical nonmagnetic bcc Fe is about 3% smaller than for ferromagnetic Fe. This conclusion was confirmed by analysis of Fe-based binary compounds.[42] This value is very close to the value $\omega_s=2.34\%$ we observed for $La(Fe_xAl_{1-x})_{13}$ and thus favors Shiga's calculations.

We can estimate the local-moment and band contribution to the thermal expansion for $La(Fe_xAl_{1-x})_{13}$ by analyzing the spontaneous and forced magnetostriction of the $x=0.89$ sample at helium temperature (see Figs. 4 and 9). Here we assume that the spin-spin correlation function in the antiferromagnetic ground state $\langle \mathbf{m}_i\cdot\mathbf{m}_j\rangle=-m_i^2$, and that the local moments do not change when the $3d$ band is polarized. Then we can calculate from $\omega_s=+1.34\%$ in the antiferromagnetic ground state and $\omega_s=+2.34\%$, $M=165$ emu/g in the induced ferromagnetic state, that $\kappa C_{\rm band}=+2.75\times10^{-8}$ cm^6/emu^2 and $\kappa C_{\rm loc}=-1.00\times10^{-8}$ cm^6/emu^2. This means that $\kappa C=+1.75\times10^{-8}$ cm^6/emu^2 for the induced ferromagnetic state and $\kappa C=-1.00\times10^{-8}$ cm^6/emu^2 in the antiferromagnetic ground state. The value of $\langle \mathbf{m}_i\cdot\mathbf{m}_j\rangle$ is clearly overestimated because of the threefold symmetry of the cubic $NaZn_{13}$ structure. A correction leads to an increase of the absolute value of $\kappa C_{\rm loc}$ and $\kappa C_{\rm band}$. An increase of the local moment at the spin-flip transition also leads to an increase of the absolute value of $\kappa C_{\rm loc}$ and $\kappa C_{\rm band}$.

The increase of the volume magnetostriction ω_s from

280 K downwards must, in our interpretation, be mainly ascribed to the increase of the local moments with decreasing temperature. It can be inferred from Fig. 4 that the magnetic contribution to the thermal expansion scales with T and not with T/T_C. Thus, the local moments start to increase or even to form from 250 K downwards, independent of the concentration x. However, the magnetic ordering temperatures show a pronounced minimum in this concentration regime ($0.81 < x < 0.89$). We believe that the minimum in magnetic ordering temperatures can be attributed to the frustration produced by the positive and negative exchange interactions.[44] This is in contrast to FeNi Invar, where it was argued that the minimum in Curie temperatures at the borderline concentration for instability of long-range ferromagnetism is due to the suppression of spin fluctuations.[45] In spin-fluctuation theory T_C is proportional to $\eta(T_C) \equiv \omega_s(T_C)/\omega_s(0)$ and in FeNi Invar this parameter $\eta(T_C)$ has a minimum in the instability regime.[45] However, one can easily see from Fig. 4 that $\eta(T_C)$ has maximum in the instability regime for $La(Fe_xAl_{1-x})_{13}$ ($x = 0.86$).

V. CONCLUSIONS

We have determined the complete magnetic phase diagram for $La(Fe_xAl_{1-x})_{13}$, consisting of a mictomagnetic, ferromagnetic, and antiferromagnetic regime. The ferromagnetic state is unstable with respect to Fe-Al-Fe superexchange in the low-iron-concentration regime, leading to mictomagnetism, and with respect to direct antiferromagnetic exchange in the high-iron-concentration regime, leading to an antiferromagnetic ground state. The existence of the antiferromagnetic state is authenticated by ac susceptibility measurements, by the metamagnetic transitions, and by extra lines in the neutron diffraction line pattern relative to the pattern of the ferromagnetic state. This unexpected occurrence of the antiferromagnetic state is explained in terms of the special crystal structure, which permits a large Fe-Fe coordination number up to 12 at small distances. Such a large Fe-Fe coordination number is only found in fcc Fe, which also is antiferromagnetic. In $La(Fe_xAl_{1-x})_{13}$ the ferromagnetic state can be recovered from the antiferromagnetic state by applying a field of a few teslas.

The room-temperature resistivity decreases with increasing iron concentration because of the decreasing potential scattering. The behavior of the low-temperature resistivity is explained in terms of the two-current model with different conductivities for the two spin currents. This model leads to an excess resistivity for the antiferromagnetic state relative to the ferromagnetic state, and explains the observed decrease of 17% of the resistivity at the spin-flip transition. This model also explains the decrease of the resistivity temperature coefficient α_r with increasing spin disorder, resulting in a positive coefficient α_r for the ferromagnetic state and a negative coefficient α_r for the antiferromagnetic and mictomagnetic state. The anomalous critical behavior of the resistivity is ascribed to the lattice softening near the Curie temperature associated with the Invar effect as proposed for Fe_3Pt by Viard and Gavoille.[35]

The spontaneous and forced volume magnetostriction are explained through a phenomenological relation between the relative volume change and the magnitude of the magnetic moments. We interpret the observed magnetovolume effects in terms of a local moment and a band effect and calculate the magnetovolume coupling constant for both the band and the local moments. This leads to a large positive value for the former and a negative value for the latter. The relative volume change $\omega_s = 2.34\%$ between 4 and 300 K for $La(Fe_{0.89}Al_{0.11})_{13}$ is close to the theoretically expected result between ferromagnetic and nonmagnetic iron $\Delta V/V = 3\%$.[43] We conclude, from the deviations from Curie-Weiss behavior in the ac susceptibility below 240 K and from the deviations from the Grüneisen function in the thermal expansion below 250 K, that magnetic short-range order sets in below 250 K and is independent of the magnetic ordering temperature, which varies from 160 to 250 K.

ACKNOWLEDGMENTS

We wish to thank F. R. de Boer of the University of Amsterdam for performing the high-field magnetization experiments and H. L. M. Bakker and R. Griessen of the Free University of Amsterdam for their hospitality and assistance with the magnetostriction experiments. The investigations carried out by the first three authors are part of the research program of the Stichting voor Fundamenteel Onderzoek der Materie (Foundation for Fundamental Research on Matter) and were made possible by financial support from the Nederlandse Organisatie voor Zuiver-Wetenschappelijk Onderzoek (Netherlands Organization for the Advancement of Pure Research).

[1]T. T. M. Palstra, J. A. Mydosh, G. J. Nieuwenhuys, A. M. van der Kraan, and K. H. J. Buschow, J. Magn. Magn. Mater. **36**, 290 (1983).

[2]T. T. M. Palstra, H. G. C. Werij, G. J. Nieuwenhuys, J. A. Mydosh, F. R. de Boer, and K. H. J. Buschow, J. Phys. F **14**, 1961 (1984).

[3]A. M. van der Kraan, K. H. J. Buschow, and T. T. M. Palstra, Hyperfine Interact. **15/16**, 717 (1983).

[4]R. D. Shull, H. Okamoto, and P. A. Beck, Solid State Commun. **20**, 863 (1976).

[5]P. Shukla and M. Wortis, Phys. Rev. B **21**, 159 (1980).

[6]R. Gersdorf, F. R. de Boer, J. C. Wolfrat, F. A. Muller, and L. W. Roeland, in *High Field Magnetism,* edited by M. Date (North-Holland, Amsterdam, 1983).

[7]G. Brändli and R. Griessen, Cryogenics **13**, 299 (1973).

[8]T. Hahn, J. Appl. Phys. **41**, 5096 (1970).

[9]B. H. Verbeek, G. J. Nieuwenhuys, H. Stocker, and J. A. Mydosh, Phys. Rev. Lett. **40**, 587 (1978).

[10]This Debye temperature was obtained from specific-heat measurements on a $x = 0.88$ sample.

[11]D. Gignoux, D. Givord, F. Givord, and R. Lemaire, J. Magn. Magn. Mater. **10**, 288 (1979).

[12]K. H. J. Buschow, Rep. Prog. Phys. **40**, 1179 (1977).

[13]T. T. M. Palstra, R. Helmholdt, A. M. van der Kraan, and K.

H. J. Buschow (unpublished).
[14]G. P. Huffman, J. Appl. Phys. **42**, 1606 (1971).
[15]M. B. Stearns, Physica **91B**, 37 (1977).
[16]L. Dobrzynski *et al.*, Solid State Commun. **46**, 217 (1983).
[17]F. Gautier, in *Magnetism of Metals and Alloys,* edited by M. Cyrot (North-Holland, Amsterdam, 1982), pp. 174—180.
[18]T. Jo, J. Phys. Soc. Jpn. **48**, 1482 (1980).
[19]T. Jo, J. Phys. Soc. Jpn. **50**, 2209 (1981).
[20]R. J. Weiss, Proc. Phys. Soc. London **82**, 281 (1963).
[21]S. Chikazumi, J. Magn. Magn. Mater. **10**, 113 (1979).
[22]W. Bendick, H. H. Ettwig, and W. Pepperhoff, J. Phys. F **8**, 2525 (1978).
[23]A. Z. Menshikov, J. Magn. Magn. Mater. **10**, 205 (1979).
[24]S. V. Vonsovskii, *Magnetism* (Wiley, New York, 1979), Vol. 2, p. 754.
[25]J. H. Mooij, Phys. Status Solidi A **17**, 521 (1973).
[26]P. B. Allen, in *Physics of Transition Metals 1980,* edited by P. Rhodes (IOP, London, 1981), p. 425.
[27]J. W. F. Dorleijn, Philips Res. Rep. **31**, 287 (1976).
[28]I. A. Campbell and A. Fert, in *Ferromagnetic Materials,* edited by E. P. Wohlfarth (North-Holland, Amsterdam, 1982), Vol. 3, p. 747.
[29]N. F. Mott, Adv. Phys. **13**, 325 (1964).
[30]W. Bendick and W. Pepperhoff, J. Phys. F **8**, 2535 (1978).
[31]P. G. de Gennes and J. Friedel, J. Phys. Chem. Solids **4**, 71 (1958).
[32]D. J. Kim, Progr. Theor. Phys. **31**, 921 (1964).
[33]M. E. Fisher and J. S. Langer, Phys. Rev. Lett. **20**, 665 (1968).
[34]M. P. Kawatra and J. I. Budnick, Int. J. Magn. **1**, 61 (1970).
[35]M. Viard and G. Gavoille, J. Appl. Phys. **50**, 1828 (1979).
[36]Y. Suezaki and H. Mori, Progr. Theor. Phys. **41**, 1177 (1969).
[37]See, for example, S. Alexander, J. S. Helman, and I. Balberg, Phys. Rev. B **13**, 304 (1976).
[38]*The Invar Problem,* edited by A. J. Freeman and M. Shimizu (North-Holland, Amsterdam, 1979).
[39]E. C. Callen and H. B. Callen, Phys. Rev. **139**, A455 (1965).
[40]E. P. Wohlfarth, J. Phys. C **2**, 68 (1969).
[41]M. Shimizu, J. Magn. Magn. Mater. **20**, 47 (1980).
[42]M. Shiga, J. Phys. Soc. Jpn. **50**, 2573 (1981).
[43]J. F. Janak and A. R. Williams, Phys. Rev. B **14**, 4199 (1976).
[44]J. C. M. van Dongen, T. T. M. Palstra, A. F. J. Morgownik, J. A. Mydosh, B. M. Geerken, and K. H. J. Buschow, Phys. Rev. B **27**, 1887 (1983).
[45]T. Morya and K. Usami, Solid State Commun. **34**, 95 (1980).